

Aromatic Interactions

Structures and Properties of Molecular Torsion Balances to Decipher the Nature of Substituent Effects on the Aromatic Edge-to-Face Interaction

Haraldur Gardarsson, W. Bernd Schweizer, Nils Trapp, and François Diederich^{*[a]}

Abstract: Various recent computational studies initiated this systematic re-investigation of substituent effects on aromatic edge-to-face interactions. Five series of Tröger base derived molecular torsion balances (MTBs), initially introduced by Wilcox and co-workers, showing an aromatic edge-to-face interaction in the folded, but not in the unfolded form, were synthesized. A fluorine atom or a trifluoromethyl group was introduced onto the edge ring in *ortho*-, *meta*-, and *para*-positions to the C–H group interacting with the face component. The substituents on the face component were varied from electron-donating to electron-withdrawing. Extensive X-ray crystallographic data allowed for a discussion on the conformational behavior of the torsional balances in the solid state. While most systems adopt the folded conformation, some were found to form supramolecular intercalative dimers, lacking the intramolecular edge-to-face interaction, which is compensated by the gain of aromatic π -stacking in-

teractions between four aryl rings of the two molecular components. This dimerization does not take place in solution. The folding free enthalpy ΔG_{fold} of all torsion balances was determined by ^1H NMR measurements by using 10 mM solutions of samples in CDCl_3 and C_6D_6 . Only the ΔG_{fold} values of balances bearing an edge-ring substituent in *ortho*-position to the interacting C–H show a steep linear correlation with the Hammett parameter (σ_{meta}) of the face-component substituent. Thermodynamic analysis using van't Hoff plots revealed that the interaction is enthalpy-driven. The ΔG_{fold} values of the balances, in addition to partial charge calculations, suggest that increasing the polarization of the interacting C–H group makes a favorable contribution to the edge-to-face interaction. The largest contribution, however, seems to originate from local direct interactions between the substituent in *ortho*-position to the edge-ring C–H and the substituted face ring.

Introduction

Noncovalent aromatic–aromatic interactions are pivotal in numerous chemical and biological processes.^[1] These interactions play a key role in host–guest chemistry,^[2] supramolecular self-assembly,^[3] stereoselective reactions,^[4] chemoselective catalysis,^[5] or protein–ligand complexation^[6] and influence the structure of biomolecules.^[7] There are three major structural motifs for aryl–aryl interactions: parallel-eclipsed, parallel-displaced, and edge-to-face (Figure 1). It is accepted that substituents affect the aryl–aryl interactions, but the exact nature of substituent effects remains a topic under investigation, both in theoretical and experimental studies.^[8]

In the 1990s, Wilcox and co-workers introduced the Tröger base derived molecular torsion balance to investigate aromatic edge-to-face interactions.^[9] This system features, in its folded state, an interaction between rings **A** and **D** (Figure 2), while the interaction is absent in the unfolded form. Atropisomerism

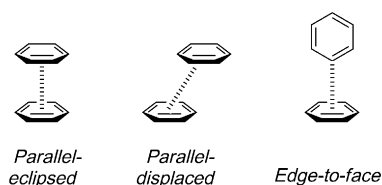


Figure 1. Aryl–aryl ring interaction motifs.

around the biaryl bond is slow on the ^1H NMR timescale, and the ratio of the folded versus the unfolded conformation is conveniently determined by integration of the signals of the methyl group at C3, yielding the folding free enthalpy ΔG_{fold} as a measure for the aromatic interaction. The Pittsburgh group studied substituent effects in CDCl_3 by using an unsubstituted phenyl ester edge ring and varying the face substituent in *para*-position to the aniline N atom. A correlation between the driving force for folding and the Hammett parameter (σ_{meta}) of the face substituent was not observed. Together with investigations on aliphatic edge moieties, this finding led the authors to the suggestion that dispersion, rather than C–H $\cdots\pi$ -type electrostatic interactions between edge and face rings, contributes to the preference of the torsion balance for the folded state.^[9b,c]

[a] H. Gardarsson, Dr. W. B. Schweizer, Dr. N. Trapp, Prof. Dr. F. Diederich
Laboratory of Organic Chemistry, ETH Zurich
Hönggerberg, HCI, 8093 Zurich (Switzerland)
Fax: (+41) 44-632-1109
E-mail: diederich@org.chem.ethz.ch

Supporting information for this article is available on the WWW under <http://dx.doi.org/10.1002/chem.201304810>.

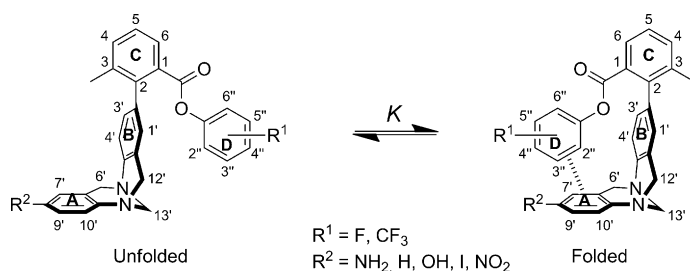


Figure 2. Schematic representation of the equilibrium between the folded (right) and unfolded (left) atropisomers of the Tröger base derived molecular torsion balance. The functional groups examined in this study as well as the numbering system used, are shown.

With sets of new Tröger base derived molecular torsion balances, we have previously quantified the weak attractive orthogonal dipolar interaction between organofluorine and amide groups^[10] and extended these investigations to the energetics of dipolar interactions between orthogonal amide groups.^[11]

During the course of our investigations on orthogonal dipolar interactions involving organofluorine, we noticed a significant substituent effect on the edge-to-face interaction in torsion balances bearing a 4-(trifluoromethyl)phenyl ester as the edge component and various electron-withdrawing (EWG) or electron-donating groups (EDG) on the face component in *para*-position to the anilino N atom.^[10a] The folding free enthalpy in C_6D_6 showed a steep linear correlation with the Hammett parameter (σ_{meta}) of the respective substituents on the face ring, with the ΔG_{fold} values becoming more negative with increasing electron-donating potency. We explained this finding with a substantial electrostatic $\text{C}-\text{H}\cdots\pi_{\text{face}}$ interaction providing the driving force for folding.^[10a] These results were in stark contrast to the work by Wilcox and co-workers described above.^[9b,c] The different results between the two studies were initially explained by Cockroft and Hunter by differences in solvation effects in C_6D_6 and CDCl_3 .^[12] A re-measurement of both sets of torsion balances in both solvents confirmed all earlier results and showed similar folding behavior in the two solvents.^[13] A steep linear free enthalpy relationship (LFER) was observed for the torsion balances with an edge-trifluoromethyl group in both C_6D_6 and CDCl_3 . No such relationship was indeed observed for the unsubstituted phenyl ester as edge component. Clearly, the additional CF_3 substituent in *ortho*-position to the interacting edge-C–H made all the difference. This finding suggested the importance of re-investigating substituent effects on the aromatic edge-to-face interaction in a comprehensive experimental study.

Additional interest in such an experimental investigation comes from recent computational studies on aryl–aryl interactions by Wheeler and Houk,^[14] Sherrill,^[15] and others.^[16] These studies suggested that the earlier, purely electrostatics-based Hunter–Sanders model^[17] is not sufficient and does not adequately describe aromatic interactions. Theoretical work by Wheeler and Houk on substituted benzene dimers indicated that all substituents, both electron-donating and electron-accepting, stabilize the parallel-eclipsed and parallel-displaced benzene dimers.^[14a,b] They concluded that through-space in-

ductive and field effects overwhelm the π -polarization effects. Sherrill and co-workers reported that direct interactions^[18] between substituents and the opposing π -system are, at least partly, responsible for substituent effects in parallel-eclipsed benzene dimers and not the change of the π -electron density in the rings.^[15b,d,e] For the aromatic edge-to-face interaction, theoretical studies mostly agree that a stabilizing effect is achieved by the introduction of an electron-withdrawing group on the edge ring, or the introduction of an electron-donating group on the face ring.^[14e,15a,16b] In the majority of these computational studies, the functional group is placed in the *para*-position of the edge C–H which interacts with the face-ring (Figure 3a). A theoretical investigation by Wheeler and Houk, on the other hand, places the edge-ring functional group in such a way that a direct interaction between this group and the π -system of the face ring is possible, similar to the situation in the Tröger base derived torsion balances investigated so far (Figure 3b, c).^[14c]

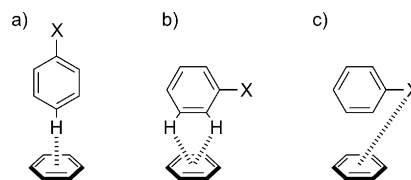


Figure 3. Edge-to-face interaction motifs used in theoretical investigations. X denotes any substituent.

Insight into the nature of aromatic edge-to-face interactions using torsional balances can be further complicated by the fact that local dipolar interactions between the dipoles of the edge and the face ring in the folded state could also affect the folding equilibrium. In a computational study, we recently demonstrated the importance of dipole orientation for the intermolecular interaction between heteroarenes stacking on peptide bonds: an antiparallel alignment of the dipoles is energetically favorable, while parallel alignment is unfavorable.^[19] In their studies utilizing molecular zippers,^[20] Hunter and co-workers already alerted to the possible energetic contribution resulting from interactions between the edge- and face-ring dipoles.^[20f,g]

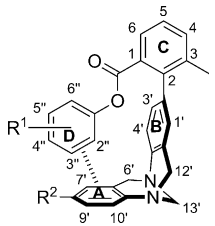
For this re-investigation into the nature of aromatic edge-to-face interactions, we synthesized 25 new molecular torsion balances and investigated their folding equilibria. Based on these data, we analyze the energetic contributions of 1) the electrostatic interaction between edge-ring C–H and the face-ring π -system, 2) direct interaction of edge-ring substituents with the substituted face ring, and 3) the interaction between the local dipoles of substituted edge and face rings. Additionally, numerous crystal structures are presented that illustrate a rather remarkable flexibility of the Tröger base scaffold.^[21]

Results and Discussion

Synthesis and solid-state structures of molecular torsion balances

The synthesis of torsion balances (\pm)-1 to (\pm)-25 (Table 1) essentially followed the protocols reported earlier.^[9a] Synthetic procedures and complete compound characterization are

Table 1. Folding free enthalpies ΔG_{fold} for fluorinated and trifluoromethylated molecular torsion balances.



	R ¹	R ²	σ_{meta} ^[a]	ΔG_{fold} [kJ mol ⁻¹] ^[b]	
				C ₆ D ₆	CDCl ₃
(\pm)-1	4''-F	NH ₂	-0.160	-3.48	-2.01
(\pm)-2	4''-F	H	0.000	-2.66	-1.78
(\pm)-3	4''-F	OH	0.121	-2.81	-1.85
(\pm)-4	4''-F	I	0.352	-2.22	-1.27
(\pm)-5	4''-F	NO ₂	0.710	-0.52	+0.01
(\pm)-6	3''-F	NH ₂	-0.160	-1.14	-0.30
(\pm)-7	3''-F	H	0.000	-1.04	-0.34
(\pm)-8	3''-F	OH	0.121	-1.01	-0.73
(\pm)-9	3''-F	I	0.352	-1.05	-0.48
(\pm)-10	3''-F	NO ₂	0.710	-0.60	-0.63
(\pm)-11	2''-F	NH ₂	-0.160	-1.75	-0.64
(\pm)-12	2''-F	H	0.000	-1.24	-0.69
(\pm)-13	2''-F	OH	0.121	-1.62	-1.08
(\pm)-14	2''-F	I	0.352	-1.77	-0.84
(\pm)-15	2''-F	NO ₂	0.710	-1.23	-1.05
(\pm)-26 ^[c]	4''-CF ₃	NH ₂	-0.160	-3.91	-2.65
(\pm)-27 ^[c]	4''-CF ₃	H	0.000	-3.47	-2.41
(\pm)-28 ^[c]	4''-CF ₃	OH	0.121	-3.46	-2.31
(\pm)-29 ^[c]	4''-CF ₃	I	0.352	-1.52	-0.61
(\pm)-30 ^[c]	4''-CF ₃	NO ₂	0.710	-0.19	+0.47
(\pm)-16	3''-CF ₃	NH ₂	-0.160	-1.00	-0.23
(\pm)-17	3''-CF ₃	H	0.000	-0.34	-0.11
(\pm)-18	3''-CF ₃	OH	0.121	-0.67	-0.38
(\pm)-19	3''-CF ₃	I	0.352	-0.49	-0.23
(\pm)-20	3''-CF ₃	NO ₂	0.710	-0.58	+0.41
(\pm)-21	2''-CF ₃	NH ₂	-0.160	-1.38	-0.20
(\pm)-22	2''-CF ₃	H	0.000	-0.89	-0.32
(\pm)-23	2''-CF ₃	OH	0.121	-1.23	-0.63
(\pm)-24	2''-CF ₃	I	0.352	-1.45	-0.82
(\pm)-25	2''-CF ₃	NO ₂	0.710	-1.26	-0.73

[a] Hammett parameters based on the ionization of substituted benzoic acids.^[28] [b] Determined by integration of the line-fitted (100% Lorentz functions) ¹H NMR spectra of 10 mM solutions at 298 K. Uncertainty ± 0.12 kJ mol⁻¹. [c] ΔG_{fold} values previously reported.^[10a,13]

given in the Supporting Information.^[29] Additionally, data for the already described systems (\pm)-26 to (\pm)-30 are included in Table 1.^[10a,13]

Crystals of several molecular torsion balances suitable for X-ray analysis were obtained by vapor diffusion of *n*-pentane into solutions of the compounds in CH₂Cl₂. All Tröger base de-

rived torsion balances crystallized until today adopted the folded form, clearly illustrating a favorable edge-to-face interaction in the solid state.^[9b,10,13] In this study, we observed the first examples of supramolecular dimers in which the edge-to-face interaction is absent.

Torsion balances (\pm)-1 (4''-F/NH₂) (the first substituent is the edge substituent labeled with respect to the ester linker in position 1'' and the second is the face-substituent in *para*-position to the anilino N-atom) and (\pm)-4 (4''-F/I) crystallize in the folded state, depicting a classic edge-to-face interaction (Supporting Information). The distance between the centroid of ring D and the calculated plane of ring A for (\pm)-4 is approximately 4.9 Å, which is similar to previously reported molecular torsion balances.^[9b,10,13] The crystal structure of (\pm)-5 (4''-F/NO₂) also shows a favorable edge-to-face interaction between rings A and D, while maintaining an interatomic distance between fluorine and nitro group that is larger than the sum of the van der Waals radii (observed $d(\text{F}\cdots\text{N})$ 3.34 Å; sum of van der Waals radii 3.02 Å; Figure 4, top).^[22]

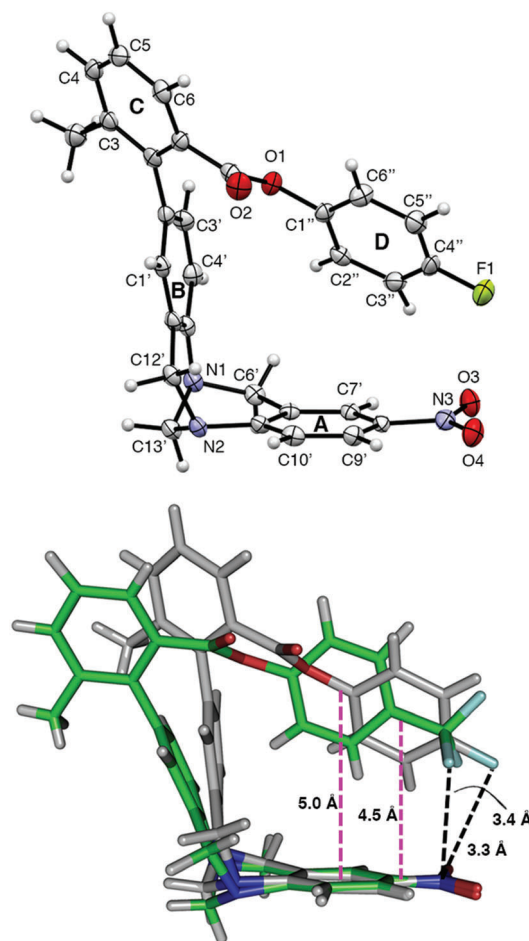


Figure 4. Top: ORTEP plot of a symmetry independent molecule of (\pm)-5 (4''-F/NO₂). Atomic displacement parameters obtained at 100 K drawn at the 50% probability level. Arbitrary numbering. Bottom: The superimposed crystal structures of (\pm)-5 (gray) and (\pm)-30 (green) (CCDC-239177).^[10a] Magenta dotted lines indicate the distance between the centroid of ring D and the calculated plane of ring A. Black dotted lines indicate the closest F \cdots N contact.

When the crystal structures of (\pm)-**5** (4''-F/NO₂) and the previously reported balance (\pm)-**30** (4''-CF₃/NO₂) (CCDC code: 239177)^[10a] are superimposed, it becomes apparent that the "hinge" angle (angle between the calculated planes of rings **A** and **B**) of the Tröger base scaffold is quite variable (Figure 4, bottom), as previously also reported by Wilcox and co-workers.^[21] By changing from a hinge angle of 116° in (\pm)-**30** to 97° for (\pm)-**5**, the interatomic distance between (the closest) fluorine and the nitro N atom becomes similar in both balances (3.34 Å for (\pm)-**5** and 3.36 Å for (\pm)-**30**). This becomes possible, since ring **D** in (\pm)-**5** moves substantially closer to ring **A** and is no longer fully perpendicular to this ring. In (\pm)-**5**, ring **D** is twisted by approximately 20° relative to its position in (\pm)-**30**. As a result of these conformational adjustments, the distance between the calculated centroid of ring **D** and the calculated plane of ring **A** changes from 4.98 Å ((\pm)-**30**) to 4.45 Å ((\pm)-**5**) (Figure 4, bottom). All symmetry-independent molecules of (\pm)-**5** show smaller inter-ring distances, as compared to (\pm)-**30** (Supporting Information).

The crystal structures of (\pm)-**10** (3''-F/NO₂), (\pm)-**15** (2''-F/NO₂), and (\pm)-**25** (2''-CF₃/NO₂) do not show an edge-to-face interaction, as supramolecular dimers form in the solid state (Figure 5 and the Supporting Information). In these dimers, the balances lose the intramolecular edge-to-face interaction, but gain three

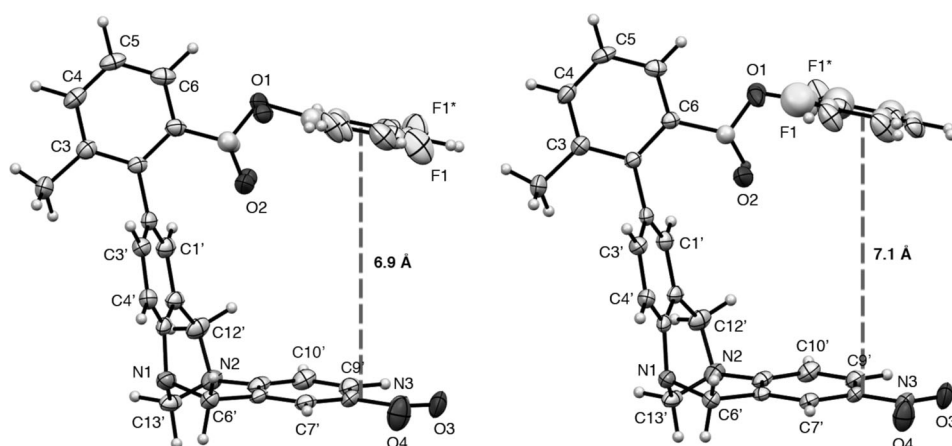


Figure 5. ORTEP plots of (\pm)-**10** (3''-F/NO₂) and (\pm)-**15** (2''-F/NO₂), left and right, respectively. Atomic displacement parameters obtained at 100 K drawn at the 50% probability level. Arbitrary numbering. For (\pm)-**10**, the fluorophenyl ring is disordered and has been refined over two positions. For (\pm)-**15**, the carboxylic group and the fluorine are disordered and have been refined over two positions. Gray dotted lines indicate the distance between the calculated centroid of ring **D** and the calculated plane of ring **A**.

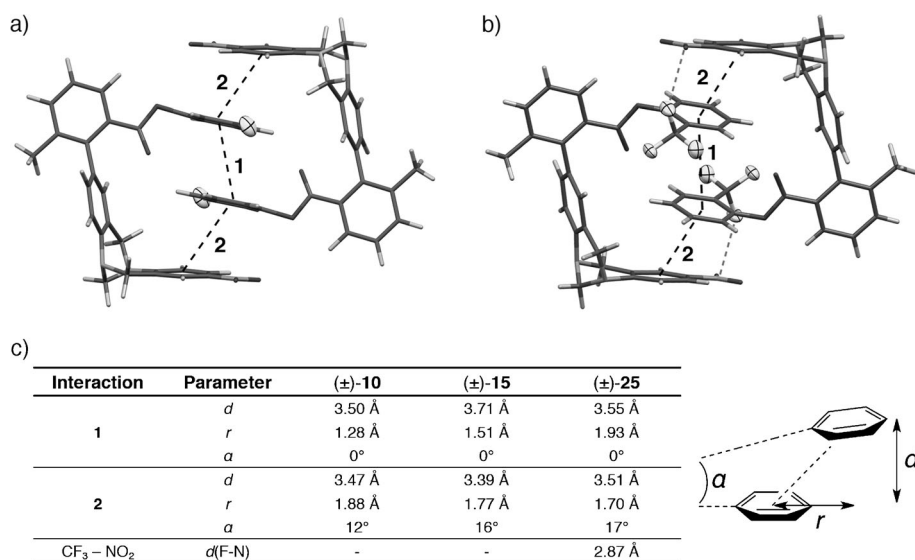


Figure 6. Dimerized structures of a) (\pm)-**10** (3''-F/NO₂) and b) (\pm)-**25** (2''-CF₃/NO₂), and c) the parameters of the parallel-displaced stacking interactions. Atomic displacement parameters of fluorine at 100 K drawn at 50% probability. Only the major conformer for (\pm)-**10** is shown for clarity. The angle α is the angle between the calculated planes of the interacting rings. Black dotted lines illustrate the favorable interactions in the dimerized structures. Gray dotted lines indicate the closest F...N contact.

intermolecular parallel-displaced aromatic interactions, as shown in Figure 6 (for the dimerized structure of (\pm)-**15** see the Supporting Information).

The extent of additional stabilization achieved by dimerization, is best illustrated by (\pm)-**25** (2''-CF₃/NO₂). The dimer causes a fluorine atom and the nitro group to come into a presumably destabilizing contact (observed *d*(F...N) 2.87 Å; sum of van der Waals radii 3.02 Å),^[22] which is overcome by the stabilization from the parallel-displaced stacking interactions (Figure 6 b). Interestingly, the isomeric molecular torsional balance (\pm)-**20** (3''-CF₃/NO₂) crystallizes as a monomer in the "normal" folded fashion (Supporting Information). Also, the crystal structures of previously reported torsional balances (\pm)-**26** (4''-CF₃/NH₂), (\pm)-**27** (4''-CF₃/H), and (\pm)-**31** (4''-CF₃/Br) all show the folded atropisomer, with an intramolecular edge-to-face interaction (Supporting Information).

Overall, this extensive X-ray analysis confirms a substantial flexibility in the Tröger base scaffold of the torsional balances, which in the folded form leads to variation in the hinge angle between its two aromatic rings **A** and **B**. Rotation around the bonds connecting the ester carboxyl to ring **C** and edge ring **D** results in a molecular tweezer-type geometry and the formation of an intercalative supramolecular dimer with

a triple parallel-shifted aromatic π -stack, a hitherto unobserved motif for stable crystal packing of Tröger base-derived torsional balances.

Folding equilibrium constants determined by ^1H NMR spectroscopy

In order to determine the folding equilibrium, the ^1H NMR spectra of each molecular torsion balance were measured as 10 mM solutions in CDCl_3 and C_6D_6 at 298 K. Prior to integration, the C3-methyl group signals were line-fitted to a 100% Lorentz function. Additional details on folding free enthalpy extraction and error analysis can be found in the Supporting Information. The folding free enthalpies (ΔG_{fold}) are summarized in Table 1.

To exclude the presence of supramolecular dimers in solution, the folding equilibrium of (\pm)-**10** was measured in CDCl_3 as a function of concentration (Figure S7 in the Supporting Information). The equilibrium is essentially independent of concentration (between 0.5 and 100.0 mM), which, along with ^1H - ^{19}F HOESY experiments (Supporting Information), indicates no dimerization in solution at the concentration used for this study (10 mM). We also conducted a molecular dynamics (MD) simulation (Figure S19 in the Supporting Information) for the fluorine series of balances, which suggests that the edge ring **D** is fully rotatable independent of the position of the F substituent. The barrier for the rotation around the ester bond to ring **D** was calculated for model systems 2''-, 3''-, and 4''-fluorophenyl acetate at the wB97XD/6-311G++(2d,p) level of theory.^[23] While the rotational barriers for 3''- and 4''-substituted derivatives were below 10 kJ mol^{-1} , the barrier for the 2''-substituted compound was calculated as 47 kJ mol^{-1} (Figure S20 in the Supporting Information), which is in agreement with the rather unhindered rotation seen in the MD study.

To analyze the substituent effects, the folding free enthalpies were plotted against the Hammett parameter (σ_{meta}) of the respective face substituent (Figures 7 and 8). The folding free enthalpy of the 4''-F series (\pm)-**1** to (\pm)-**5** shows a steep linear correlation with the Hammett parameter, with ΔG_{fold} values becoming more negative upon moving to electron-donating substituents (Figure 7), which was also reported for the 4''- CF_3 MTB series.^[10a, 13] At the time, this correlation was contributed to an edge-to-face interaction strongly modulated by electrostatic contribution from the $\text{C}-\text{H}\cdots\pi_{\text{face}}$ contact. The folding equilibria of 2''-F and 3''-F torsion balances ((\pm)-**6** to (\pm)-**15**) are nearly independent of the face-ring substituent (Figure 7). All balances, however, that contain a hydrogen or iodine atom on the face-ring, show ΔG_{fold} values in C_6D_6 which are different than expected. As predicted by theoretical work by Wheeler and Houk,^[14c] this is probably due to the small, for hydrogen, and large, for iodine, dispersion contribution to the edge-to-face interaction. The folding in the 2''-F series is consistently more favorable compared to the 3''-F series. The same trend is observed for the trifluoromethylated series (2''- and 3''- CF_3). The reasons for this are, as yet, unclear. The desolvation model postulated by Hunter and Cockcroft^[12] cannot explain the aforementioned results, as all molecular torsion balances now con-

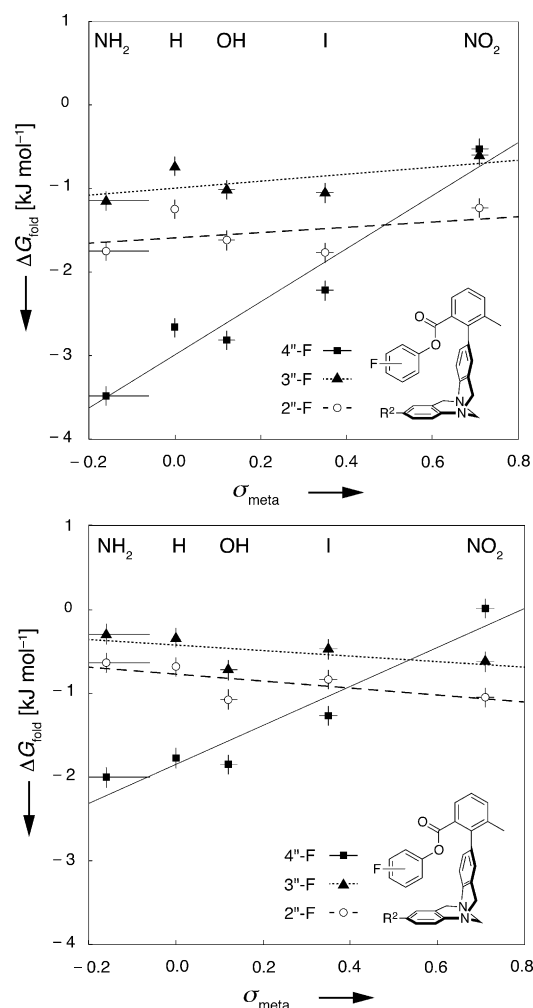


Figure 7. Folding free enthalpies ΔG_{fold} of molecular torsion balances (\pm)-**1** to (\pm)-**15** in C_6D_6 (top) and CDCl_3 (bottom) at 298 K plotted against the respective Hammett parameter (σ_{meta}) of substituent R^2 .

tain a polarizing fluorine or a trifluoromethyl group on the edge-ring. Recently, Cockcroft and co-workers have examined the desolvation of substituents.^[24] Although desolvation could be involved in the modulation of the folding free enthalpy within a series (e.g., (\pm)-**1** to (\pm)-**5**), this approach is inadequate to describe the differences between the 2''-, 3''-, and 4''-substituted series, as they contain identical substituents.

The folding equilibrium in the 4''- CF_3 series is affected to a greater extent by the nature of the face substituent than in the 4''-F series (Figure 8). Upon changing from (\pm)-**30** (4''- CF_3/NO_2) to (\pm)-**26** (4''- CF_3/NH_2), the ΔG_{fold} value in deuterated benzene changes by -3.72 kJ mol^{-1} , whereas moving from (\pm)-**5** (4''-F/ NO_2) to (\pm)-**1** (4''-F/ NH_2), the free enthalpy difference amounts to -2.96 kJ mol^{-1} . As aryl-bound fluorine exerts a stronger polarization effect than an aryl-bound trifluoromethyl group on hydrogens *ortho* to the substituent (see below), polarization alone is not enough to explain these folding data. A stronger direct interaction between the CF_3 group and the face-ring π -system, which adds to the polarization effect, could explain these results.

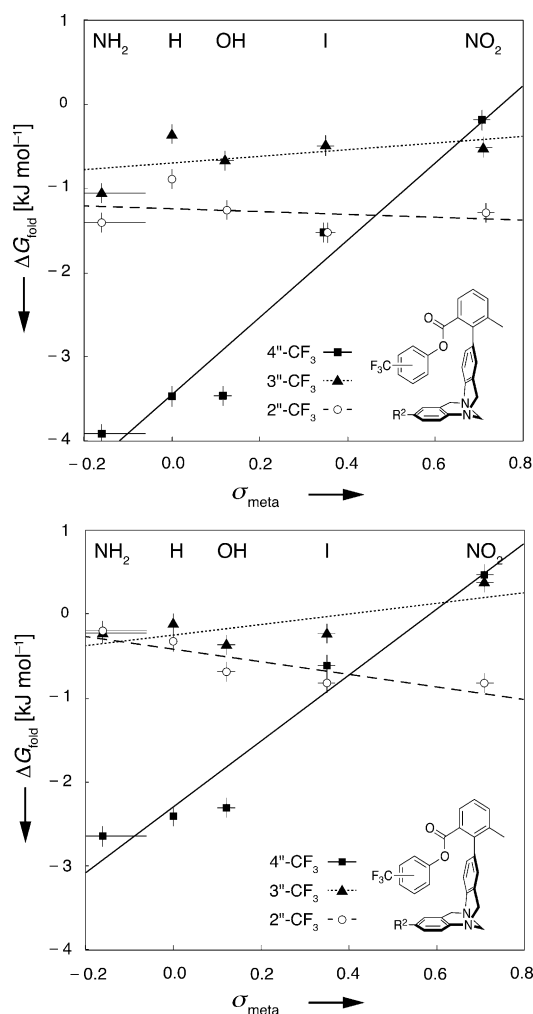


Figure 8. Folding free enthalpies ΔG_{fold} of molecular torsion balances (\pm)-16 to (\pm)-30 in C_6D_6 (top) and CDCl_3 (bottom) at 298 K plotted against the respective Hammett parameter (σ_{meta}) of substituent R^2 . The data for the 4''- CF_3 series have been taken from previous publications.^[10a,13] The data point for (\pm)-29 (4''- CF_3/I) has been shifted slightly from $\sigma_{\text{meta}} = 0.352$ to 0.345, to avoid complete overlap with the data point for (\pm)-24 (2''- CF_3/I).

Calculated dipoles and partial charges

We estimated the partial charges of the hydrogen atoms in the F- and CF_3 -substituted edge ring **D** of the torsion balances by performing calculations at the MP2/aug-cc-pVDZ//wB97XD/6-311G++(2d,p) level of theory^[23,25] for the respective constitutionally isomeric fluorophenyl and trifluoromethylphenyl acetates (Supporting Information) as model systems for the edge-part of the molecular torsion balances. Using the ESP grid-based method (CHELPG),^[26] we obtained a good correlation between calculated and experimental dipole moments (Supporting Information), which had previously been reported using other theoretical methods.^[27] Figure 9a depicts the calculated point charges for 5''-H (for partial charges of all edgering hydrogens, see Table S11 in the Supporting Information).

In both the F- and CF_3 -edge series, the extent of polarization is as expected. The positive partial charge on 5''-H is the highest for 4''-substituted arenes, while the 2''- and 3''-substituted

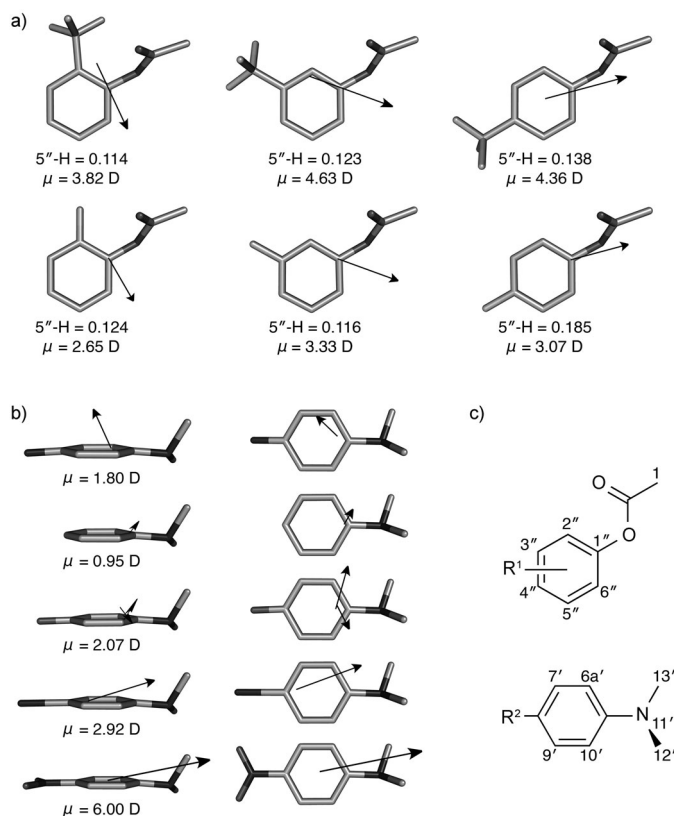


Figure 9. a) Calculated ESP (CHELPG) partial charges and the corresponding dipole moments of trifluoromethylated and fluorinated phenyl acetates as model systems for the edge-component. The dihedral angles (φ) $\text{C}2''\text{-C}1''\text{-O-C(O)}$ and $\text{C}1''\text{-O-C(O)-C}1$ were restricted to -117.3° and 174.4° , respectively. b) Calculated dipoles of 4-substituted (from top: NH_2 , H, OH, I, NO_2) N,N -dimethylanilines as model systems for the face-component in the torsional balances. Level of theory MP2/aug-cc-pVDZ//wB97XD/6-311G++(2d,p) for all structures except for the iodinated model system, where the MP2/LANL2DZ//wB97XD/LANL2DZ level of theory was used. Two arrows indicate the dipole of the hydroxy-containing model system after a 180° rotation of the hydroxy moiety. During optimization, parameters were restricted to mimic the Tröger base backbone. $\angle(\text{C}8\text{-C}10\text{a}'\text{-N}11') = 175.8^\circ$, $\angle(\text{C}6\text{a}'\text{-C}10\text{a}'\text{-N}11') = 121.3^\circ$, $\angle(\text{C}10\text{a}'\text{-N}11'\text{-C}13') = 110.2^\circ$, $\angle(\text{C}10\text{a}'\text{-N}11'\text{-C}12') = 113.4^\circ$, $\varphi(\text{C}6\text{a}'\text{-C}10\text{a}'\text{-N}11'\text{-C}13') = -15.3^\circ$, and $\varphi(\text{C}6\text{a}'\text{-C}10\text{a}'\text{-N}11'\text{-C}12') = 105.5^\circ$. Values were averaged from crystal structures in this manuscript showing an edge-to-face interaction. c) Indicates the numbering system of the edge- and face-components.

derivatives show similar partial charges (Figure 9a). The calculated partial charges, however, do not explain, why the correlation of ΔG_{fold} values with the Hammett parameter is steeper in the 4''- CF_3 than in the 4''-F series. Clearly, the polarization of 5''-H, which interacts with the face ring, is not the only contributor to the modulation of the folding free enthalpies by the substituents on the face ring.

Two possible explanations can be offered. Firstly, there is a local direct interaction between the edge-substituent at position 4'' and the face-component π -system, which is larger for the more spacious 4''- CF_3 group than for fluorine. Secondly, a substantial part of the substituent effect is due to interaction between the local dipoles of the interacting rings (Figure 9a, b).^[19] The local dipole moments for models of the edge ring and the face ring (4-substituted N,N -dimethylanilines) were cal-

culated at the MP2/aug-cc-pVDZ//wb97xd/6-311G++(2d,p) level of theory, except for the iodinated compound, for which MP2/LANL2DZ//wb97xd/LANL2DZ was used (Figure 9b). To get a closer approximation of the dipoles in the molecular torsion balances, several restraints were applied during optimization (Figure 9). The model calculations suggest that in the substituted torsion balances with 4''-F- or 4''-CF₃-substituents at the edge ring, the interacting dipoles are aligned in an unfavorable, nearly parallel fashion for the NO₂-substituted face ring, whereas they become increasingly orthogonal and therefore more favorable when the face-ring is donor-substituted, in particular in the NH₂ case. However, the fact that there is relatively little change in the folding free enthalpy for the 2''- and 3''-substituted torsion balances despite strongly different local dipole-dipole interactions suggests that dipolar interactions alone are not sufficient to explain the substituent effect. At this point, our joint experimental/computational analysis points to larger contributions to the substituent effects in aromatic edge-to-face interactions from local direct substituent interactions and minor contributions from both the electrostatic interactions between the polarized 5''-H atom and the substituted face ring, and from local dipole-dipole interactions.

Thermodynamic analysis by variable-temperature NMR (VT-NMR) measurements

All F-substituted molecular torsion balances ((±)-1 to (±)-15) were subjected to variable-temperature NMR (VT-NMR) studies, followed by van't Hoff plot analysis, in order to extract the enthalpic (ΔH) and entropic term ($-T\Delta S$) for the folding process (Figure 10). For further details on the VT-NMR experiments and van't Hoff plots, see the Supporting Information.

As expected, the folding enthalpy for the 4''-fluorinated series ((±)-1 to (±)-5) becomes more favorable as the electron density of the face-ring is increased (Figure 10, left). As the degrees of freedom are reduced upon folding, the entropic term becomes increasingly unfavorable. The overall result is a small gain in ΔG_{fold} as the electron density of ring A is increased. In the 4''-edge-ring substituted series, the enthalpic gain is small-

er when the face ring is unsubstituted ((±)-2), than for both the amino- and hydroxy-substituted systems ((±)-1 and (±)-3). This could be due to the dispersion interactions mentioned earlier, or indicative of a direct interaction between fluorine and the substituents on ring A. The thermodynamic quantities of 3''- and 2''-edge-ring fluorinated torsion balances do not change with the nature (EWG or EDG) of the face-substituent. These results further support the fact that the dominant factor in the substituent effect seen for the 4''-F series is the local direct interaction between the edge substituent and the substituted face component.

Conclusion

We have synthesized 25 new molecular torsion balances and examined their folding equilibrium in the ambitious attempt to provide an experimental study on the nature of substituent effects on edge-to-face interactions, which have been addressed in broad, recent computational analysis. We first investigated in detail the structural properties of the balances in the solid state and in the majority of the crystal structures observed a preference for the folded conformation. Conformational flexibility is visible in the Tröger base component, which can adopt hinge angles between its two aromatic rings varying from 97 to 116°, in agreement with previous findings by the Wilcox group.^[21] Furthermore, some solid-state structures also reveal different conformations of the carboxylated edge ring, shaping a cleft for intercalative supramolecular dimer formation. This dimerization however, is not observed in solution.

Folding analysis by ¹H NMR spectroscopy clearly revealed that only balances bearing a 4''-edge-ring substituent show a steep linear correlation with the Hammett parameter of the face substituent. No such modulation of the driving force for folding by face substituents was observed in the 2''- and 3''-edge-substituted systems. Also, folding in the 2''-substituted series is consistently preferred over the folding in the 3''-substituted series. These conclusions were further supported by VT-NMR studies, followed by van't Hoff analysis. To explain these experimental results, theoretical calculations at a high

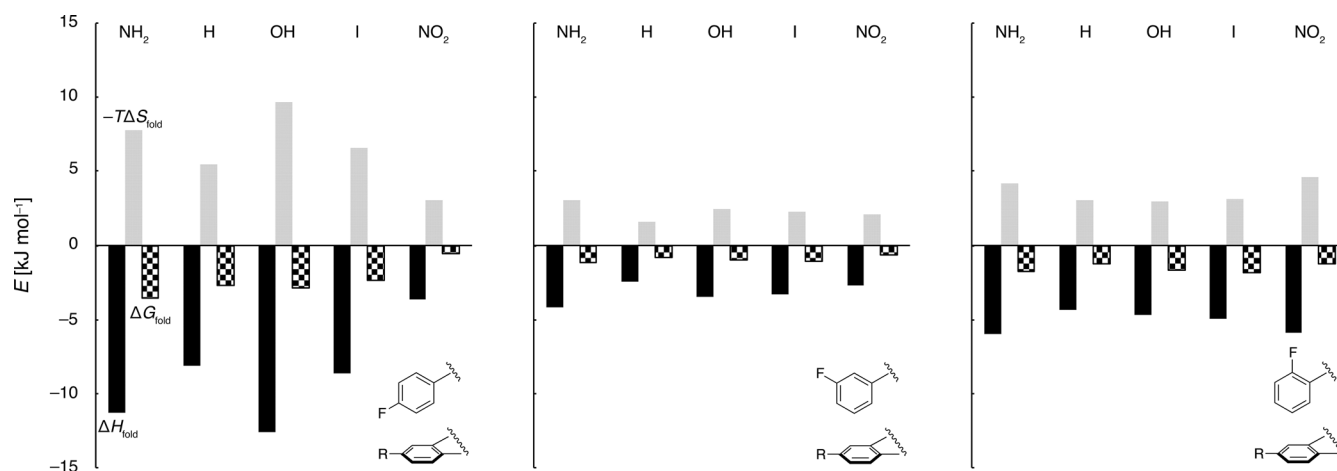


Figure 10. Thermodynamic quantities from VT-NMR of molecular torsion balances ((±)-1 to (±)-5 (left), (±)-6 to (±)-10 (middle), and (±)-11 to (±)-15 (right)). Black = ΔH_{fold} ; gray = $-T\Delta S_{\text{fold}}$; checkered = ΔG_{fold} .

level of theory were carried out on model systems for the edge- and face rings in the balances and based on the combined experimental/computational data, we draw the following conclusions.

- 1) The electrostatic component resulting from the edge C–H $\cdots\pi_{\text{face}}$ interaction is apparent in the comparison between the folding free enthalpies of the 4''-substituted series versus the 2''- and 3''-series, but does not seem the major contributor to the driving force for folding.
 - 2) A major part of ΔG_{fold} presumably originates from direct interactions of the 4''-F and 4''-CF₃ on the edge ring with the enhanced π -electron density of the face component upon changing its substituent from NO₂ to NH₂. This is in agreement with recent computational predictions.^[14a,c,e-h,15b-f]
 - 3) The interaction of the local dipoles of the edge- and face-ring dipoles can be further invoked to explain the steep linear correlation in the 4''-substituted edge-ring series, but the fact that the folding in the 2''- and 3''-F or the corresponding CF₃ series is largely independent of the face substituent, casts doubt on the importance of this local dipole–dipole interaction.
- The folding equilibria of the described torsion balances suggest that the modulation by the face substituent most likely stems from local direct interactions between the 4''-substituent and the face component π -system and its substituent.

Acknowledgements

We acknowledge the ETH Research Council and F. Hoffmann-La Roche Ltd., Basel for funding and Dr. Aaron D. Finke for help with the X-ray crystal structures.

Keywords: aromatic edge-to-face interactions · dipole–dipole interactions · fluorine · molecular torsion balance · substituent effects · Tröger base

- [1] a) E. A. Meyer, R. K. Castellano, F. Diederich, *Angew. Chem.* **2003**, *115*, 1244–1287; *Angew. Chem. Int. Ed.* **2003**, *42*, 1210–1250; b) L. M. Salonen, M. Ellermann, F. Diederich, *Angew. Chem.* **2011**, *123*, 4908–4944; *Angew. Chem. Int. Ed.* **2011**, *50*, 4808–4842.
- [2] a) L. Mosca, P. Koutník, V. M. Lynch, G. V. Zyryanov, N. A. Esipenko, P. Anzenbacher Jr., *Cryst. Growth Des.* **2012**, *12*, 6104–6109; b) F.-G. Klärner, T. Schrader, *Acc. Chem. Res.* **2013**, *46*, 967–978; c) H.-J. Schneider, *Acc. Chem. Res.* **2013**, *46*, 1010–1019.
- [3] a) C. G. Claessens, J. F. Stoddart, *J. Phys. Org. Chem.* **1997**, *10*, 254–272; b) H.-J. Schneider, *Angew. Chem.* **2009**, *121*, 3982–4036; *Angew. Chem. Int. Ed.* **2009**, *48*, 3924–3977.
- [4] a) G. Santoni, M. Mba, M. Bonchio, W. A. Nugent, C. Zonta, G. Licini, *Chem. Eur. J.* **2010**, *16*, 645–654; b) E. H. Krenske, K. N. Houk, *Acc. Chem. Res.* **2013**, *46*, 979–989.
- [5] H. Nakajima, M. Yasuda, R. Takeda, A. Baba, *Angew. Chem.* **2012**, *124*, 3933–3936; *Angew. Chem. Int. Ed.* **2012**, *51*, 3867–3870.
- [6] A. Di Fenza, A. Heine, U. Koert, G. Klebe, *ChemMedChem* **2007**, *2*, 297–308.
- [7] a) S. K. Burley, G. A. Petsko, *Adv. Protein Chem.* **1988**, *39*, 125–189; b) S. K. Burley, G. A. Petsko, *Trends Biotechnol.* **1989**, *7*, 354–359; c) E. Lanzarotti, R. R. Biekofsky, D. A. Estrin, M. A. Marti, A. G. Turjanski, *J. Chem. Inf. Model.* **2011**, *51*, 1623–1633; d) K. E. Riley, P. Hobza, *Acc. Chem. Res.* **2013**, *46*, 927–936.
- [8] a) F. Cozzi, M. Cinquini, R. Annunziata, T. Dwyer, J. S. Siegel, *J. Am. Chem. Soc.* **1992**, *114*, 5729–5733; b) F. Cozzi, M. Cinquini, R. Annunziata, J. S. Siegel, *J. Am. Chem. Soc.* **1993**, *115*, 5330–5331; c) F. Cozzi, F. Ponzini, R. Annunziata, M. Cinquini, J. S. Siegel, *Angew. Chem.* **1995**, *107*, 1092–1094; *Angew. Chem. Int. Ed. Engl.* **1995**, *34*, 1019–1020; d) F. Cozzi, J. S. Siegel, *Pure Appl. Chem.* **1995**, *67*, 683–689; e) M. J. Rashkin, M. L. Waters, *J. Am. Chem. Soc.* **2002**, *124*, 1860–1861; f) B. W. Gung, M. Patel, X. Xue, *J. Org. Chem.* **2005**, *70*, 10532–10537; g) B. W. Gung, X. Xue, H. J. Reich, *J. Org. Chem.* **2005**, *70*, 3641–3644; h) X. Mei, C. Wolf, *J. Org. Chem.* **2005**, *70*, 2299–2305; i) S. E. Snyder, P. I. Volkers, D. A. Engebretson, W. Lee, W. H. Pirkle, J. R. Carey, *Org. Lett.* **2007**, *9*, 2341–2343; j) F. Cozzi, R. Annunziata, M. Benaglia, K. K. Baldrige, G. Aguirre, J. Estrada, Y. Sritana-Anant, J. S. Siegel, *Phys. Chem. Chem. Phys.* **2008**, *10*, 2686–2694; k) B. W. Gung, B. U. Emenike, C. N. Alvarez, J. Rakovan, K. Kirschbaum, N. Jain, *Tetrahedron Lett.* **2010**, *51*, 1648–1650; l) C. R. Martinez, B. L. Iverson, *Chem. Sci.* **2012**, *3*, 2191–2201; m) S. E. Snyder, B.-S. Huang, Y.-T. Chen, H.-S. Lin, J. R. Carey, *Org. Lett.* **2012**, *14*, 3442–3445; n) J. L. Xia, S. H. Liu, F. Cozzi, M. Mancinelli, A. Mazzanti, *Chem. Eur. J.* **2012**, *18*, 3611–3620; o) W. B. Jennings, N. O'Connell, J. F. Malone, D. R. Boyd, *Org. Biomol. Chem.* **2013**, *11*, 5278–5291.
- [9] a) T. H. Webb, C. S. Wilcox, *J. Org. Chem.* **1990**, *55*, 363–365; b) S. Paliwal, S. Geib, C. S. Wilcox, *J. Am. Chem. Soc.* **1994**, *116*, 4497–4498; c) E.-i. Kim, S. Paliwal, C. S. Wilcox, *J. Am. Chem. Soc.* **1998**, *120*, 11192–11193.
- [10] a) F. Hof, D. M. Scofield, W. B. Schweizer, F. Diederich, *Angew. Chem.* **2004**, *116*, 5166–5169; *Angew. Chem. Int. Ed.* **2004**, *43*, 5056–5059; b) F. R. Fischer, W. B. Schweizer, F. Diederich, *Angew. Chem.* **2007**, *119*, 8418–8421; *Angew. Chem. Int. Ed.* **2007**, *46*, 8270–8273.
- [11] F. R. Fischer, P. A. Wood, F. H. Allen, F. Diederich, *Proc. Natl. Acad. Sci. USA* **2008**, *105*, 17290–17294.
- [12] a) S. L. Cockroft, C. A. Hunter, *Chem. Commun.* **2006**, 3806–3808; b) S. L. Cockroft, C. A. Hunter, *Chem. Commun.* **2009**, 3961–3963.
- [13] F. R. Fischer, W. B. Schweizer, F. Diederich, *Chem. Commun.* **2008**, 4031–4033.
- [14] a) S. E. Wheeler, K. N. Houk, *J. Am. Chem. Soc.* **2008**, *130*, 10854–10855; b) S. E. Wheeler, K. N. Houk, *J. Chem. Theory Comput.* **2009**, *5*, 2301–2312; c) S. E. Wheeler, K. N. Houk, *Mol. Phys.* **2009**, *107*, 749–760; d) S. E. Wheeler, A. J. McNeil, P. Müller, T. M. Swager, K. N. Houk, *J. Am. Chem. Soc.* **2010**, *132*, 3304–3311; e) R. K. Raju, J. W. G. Bloom, Y. An, S. E. Wheeler, *ChemPhysChem* **2011**, *12*, 3116–3130; f) S. E. Wheeler, *J. Am. Chem. Soc.* **2011**, *133*, 10262–10274; g) S. E. Wheeler, *CrystEngComm* **2012**, *14*, 6140–6145; h) S. E. Wheeler, *Acc. Chem. Res.* **2013**, *46*, 1029–1038.
- [15] a) M. O. Sinnokrot, C. D. Sherrill, *J. Am. Chem. Soc.* **2004**, *126*, 7690–7697; b) A. L. Ringer, M. O. Sinnokrot, R. P. Lively, C. D. Sherrill, *Chem. Eur. J.* **2006**, *12*, 3821–3828; c) M. O. Sinnokrot, C. D. Sherrill, *J. Phys. Chem. A* **2006**, *110*, 10656–10668; d) S. A. Arnstein, C. D. Sherrill, *Phys. Chem. Chem. Phys.* **2008**, *10*, 2646–2655; e) A. L. Ringer, C. D. Sherrill, *J. Am. Chem. Soc.* **2009**, *131*, 4574–4575; f) E. G. Hohenstein, J. Duan, C. D. Sherrill, *J. Am. Chem. Soc.* **2011**, *133*, 13244–13247; g) C. D. Sherrill, *Acc. Chem. Res.* **2013**, *46*, 1020–1028.
- [16] a) J. Ribas, E. Cubero, F. J. Luque, M. Orozco, *J. Org. Chem.* **2002**, *67*, 7057–7065; b) E. C. Lee, B. H. Hong, J. Y. Lee, J. C. Kim, D. Kim, Y. Kim, P. Tarakeshwar, K. S. Kim, *J. Am. Chem. Soc.* **2005**, *127*, 4530–4537; c) K. E. Riley, K. M. Merz Jr., *J. Phys. Chem. B* **2005**, *109*, 17752–17756; d) S. Tsuzuki, K. Honda, T. Uchimaru, M. Mikami, *J. Chem. Phys.* **2006**, *125*, 124304; e) S. Tsuzuki, T. Uchimaru, *Curr. Org. Chem.* **2006**, *10*, 745–762.
- [17] a) C. A. Hunter, J. K. M. Sanders, *J. Am. Chem. Soc.* **1990**, *112*, 5525–5534; b) C. A. Hunter, J. Singh, J. M. Thornton, *J. Mol. Biol.* **1991**, *218*, 837–846; c) C. A. Hunter, *Angew. Chem.* **1993**, *105*, 1653–1655; *Angew. Chem. Int. Ed. Engl.* **1993**, *32*, 1584–1586; d) C. A. Hunter, *Chem. Soc. Rev.* **1994**, *23*, 101–109; e) C. A. Hunter, K. R. Lawson, J. Perkins, C. J. Urch, *J. Chem. Soc. Perkin Trans. 2* **2001**, 651–669.
- [18] In this study, we define as direct interaction the interaction between edge substituents and the (substituted)face component. For various refinements of this definition see references [14a,c,e,15b,e,f].
- [19] M. Harder, B. Kuhn, F. Diederich, *ChemMedChem* **2013**, *8*, 397–404.
- [20] a) A. P. Bisson, F. J. Carver, C. A. Hunter, J. P. Waltho, *J. Am. Chem. Soc.* **1994**, *116*, 10292–10293; b) H. Adams, F. J. Carver, C. A. Hunter, J. C.

- Morales, E. M. Seward, *Angew. Chem.* **1996**, *108*, 1628–1631; *Angew. Chem. Int. Ed. Engl.* **1996**, *35*, 1542–1544; c) F. J. Carver, C. A. Hunter, E. M. Seward, *Chem. Commun.* **1998**, 775–776; d) H. Adams, J.-L. J. Blanco, G. Chessari, C. A. Hunter, C. M. R. Low, J. M. Sanderson, J. G. Vinter, *Chem. Eur. J.* **2001**, *7*, 3494–3503; e) H. Adams, C. A. Hunter, K. R. Lawson, J. Perkins, S. E. Spey, C. J. Urch, J. M. Sanderson, *Chem. Eur. J.* **2001**, *7*, 4863–4878; f) F. J. Carver, C. A. Hunter, P. S. Jones, D. J. Livingstone, J. F. McCabe, E. M. Seward, P. Tiger, S. E. Spey, *Chem. Eur. J.* **2001**, *7*, 4854–4862; g) F. J. Carver, C. A. Hunter, D. J. Livingstone, J. F. McCabe, E. M. Seward, *Chem. Eur. J.* **2002**, *8*, 2847–2859; h) G. Chessari, C. A. Hunter, C. M. R. Low, M. J. Packer, J. G. Vinter, C. Zonta, *Chem. Eur. J.* **2002**, *8*, 2860–2867; i) S. L. Cockroft, C. A. Hunter, K. R. Lawson, J. Perkins, C. J. Urch, *J. Am. Chem. Soc.* **2005**, *127*, 8594–8595; j) S. L. Cockroft, C. A. Hunter, *Chem. Soc. Rev.* **2007**, *36*, 172–188; k) S. L. Cockroft, J. Perkins, C. Zonta, H. Adams, S. E. Spey, C. M. R. Low, J. G. Vinter, K. R. Lawson, C. J. Urch, C. A. Hunter, *Org. Biomol. Chem.* **2007**, *5*, 1062–1080.
- [21] I. Sucholeiki, V. Lynch, L. Phan, C. S. Wilcox, *J. Org. Chem.* **1988**, *53*, 98–104.
- [22] A. Bondi, *J. Phys. Chem.* **1964**, *68*, 441–451.
- [23] J.-D. Chai, M. Head-Gordon, *J. Chem. Phys.* **2008**, *128*, 084106.
- [24] a) I. K. Mati, C. Adam, S. L. Cockroft, *Chem. Sci.* **2013**, *4*, 3965–3972; b) K. B. Muchowska, C. Adam, I. K. Mati, S. L. Cockroft, *J. Am. Chem. Soc.* **2013**, *135*, 9976–9979; c) L. Yang, C. Adam, G. S. Nichol, S. L. Cockroft, *Nat. Chem.* **2013**, *5*, 1006–1010.
- [25] M. Head-Gordon, J. A. Pople, M. J. Frisch, *Chem. Phys. Lett.* **1988**, *153*, 503–506.
- [26] C. M. Breneman, K. B. Wiberg, *J. Comput. Chem.* **1990**, *11*, 361–373.
- [27] a) F. Martin, H. Zipse, *J. Comput. Chem.* **2005**, *26*, 97–105; b) G. S. Maciel, E. Garcia, *Chem. Phys. Lett.* **2005**, *409*, 29–33.
- [28] C. Hansch, A. Leo, R. W. Taft, *Chem. Rev.* **1991**, *91*, 165–195.
- [29] CCDC-957749 ((±)-**31**), CCDC-957750 ((±)-**27**), CCDC-957751 ((±)-**26**), CCDC-957752 ((±)-**5**), CCDC-957753 ((±)-**10**), CCDC-957754 ((±)-**20**), CCDC-957755 ((±)-**1**), CCDC-957756 ((±)-**4**), CCDC-957757 ((±)-**15**), and CCDC-957758 ((±)-**25**) contain the supplementary crystallographic data for this paper. These data can be obtained free of charge from The Cambridge Crystallographic Data Centre via www.ccdc.cam.ac.uk/data_request/cif.

Received: December 9, 2013

Published online on ■ ■ ■ ■, 0000

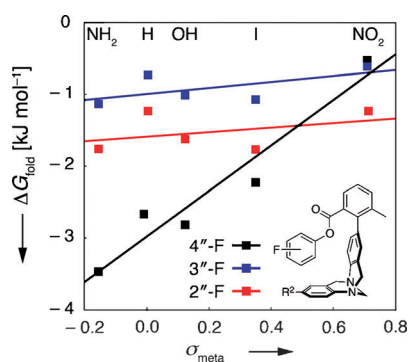
FULL PAPER

Aromatic Interactions

H. Gardarsson, W. B. Schweizer, N. Trapp,
F. Diederich*



Structures and Properties of Molecular
Torsion Balances to Decipher the
Nature of Substituent Effects on the
Aromatic Edge-to-Face Interaction



Direct interactions dominate: The importance of local direct interactions in the edge-to-face interaction was examined with a large library of Tröger base derived molecular torsion balances. Modulation of the folding free enthalpy is only observed when edge-ring substituents are capable of directly interacting with the face-ring π system (see figure). Experimental results and theoretical calculations indicate that local direct interactions make the largest contribution to substituent effects in the edge-to-face aromatic interactions.